

# The Design and Use of a Cone Chromaticity Space: A Tutorial

*Colorimetric data as revised by Judd can be transformed to König fundamentals L, M, S, representative of the long- (LWS), middle- (MWS), and short- (SWS) wavelength sensitive cone spectral sensitivities. The fundamentals are normalized so that two cone types, M and L, sum to the luminous efficiency function,  $Y_J$ . The height of the S fundamental is undefined in this transformation. A constant luminance chromaticity plane can be derived by calculating  $L/Y_J$  and  $S/Y_J$ , with the area of S set equal to that of  $Y_J$ . This chromaticity space is convenient for calculations of real stimuli. The axes of this space, when adjusted to reflect cone adaptation to the equal-energy spectrum have been shown to match the null axes of the major retino-cortical processing streams. The relative cone troland chromaticities can be multiplied by the retinal illuminance level to give L, M, and S trolands. In this metric, chromaticity data can be plotted as threshold-vs.-illuminance functions. Cone excitation is derived from cone trolands, by dividing by the maximal sensitivity of the fundamentals. Cone excitation units are used to derive models of retinal processing. The cone quantal excitation rate is a scaled version of the cone excitation.*

© 1996 John Wiley & Sons, Inc.

*Key words: colorimetry, color space, chromaticity space, König fundamentals, cone excitation.*

## INTRODUCTION

A cone chromaticity space is a transform of a colorimetric specification system into coordinates that represent cone stimulation. The concept of cone chromaticity spaces dates to Maxwell<sup>1</sup> and Schrödinger,<sup>2</sup> but is only recently starting to see use. In early approaches, the three cone stimulation levels were viewed as three vectors ris-

ing from a zero luminance origin. The chromaticity diagram was plotted as an equilateral triangle, with the three cone peak stimulations at its apices and equal energy white as its center of gravity. Although this approach may seem intuitive and has been used in the development of a uniform chromaticity diagram,<sup>3</sup> it is hard to work in such a geometrical space.

MacLeod and Boynton<sup>4</sup> in 1979 created a rectangular cone chromaticity diagram that presented an equal luminance plane. A similar proposal had been put forth by Luther<sup>5</sup> in 1927. The MacLeod-Boynton diagram is a projective transformation obeying center-of-gravity rules. Additionally, it allows very easy computation of predicted metamers and calculations of cone equations. In this tutorial, we review how this type of cone chromaticity space is derived, some of its properties, and how it can be used.

## KÖNIG FUNDAMENTALS

The first step in deriving a cone chromaticity space is the transform of colorimetric values into a new primary set representative of the spectral sensitivities of the human cone photoreceptors. With the definition of trichromacy came the recognition<sup>1,6</sup> that a transformation from color matching to the "fundamentals" should exist. Since there is an infinite number of possible transformations, the problem is how to constrain the transformation. An approach that is now widely used is one that uses the data of hereditary color defect. Color defects have been studied since the 1800s.<sup>7</sup> The most common forms, occurring primarily in males, are called protan and deutan defects.<sup>7</sup> A less common form occurring equally in males and females is called the tritan defect. Color matching can be dichromatic or trichromatic. A dichromat is an observer who requires only two primaries for full spectrum color matching. König, a student of Helmholtz, proposed an interpretation of hereditary dichromacy as a



reduction of normal trichromacy.<sup>8,9</sup> Fundamentals using the data of dichromats are termed König fundamentals. Today König fundamentals are explicitly linked to the spectral sensitivities of the human cone photoreceptors.<sup>10,11</sup>

To derive König fundamentals, the dichromatic color matches are treated as a reduction from normal trichromatic color matching. The dichromatic color-matching data are normalized as for the trichromat, and can then be represented on a chromaticity diagram by connecting the test wavelength to the matching primary mixture. The resulting lines, termed confusion lines, connect the dichromatic metamers. Confusion lines converge at a point in chromaticity space, called the copunctal point. The three copunctal points, each representing the spectral sensitivity of the "missing" fundamental of protanopes, deuteranopes, and tritanopes, define the three cone-based physiological primaries **L**, **M**, and **S**. These fundamentals have the spectral sensitivity of the long-wavelength-, middle-wavelength-, and short-wavelength-sensitive (LWS, MWS, SWS) cones.

While the copunctal points uniquely define the spectral sensitivities of the cone photoreceptors, there remains a free choice for normalization. There are two intuitive choices. The heights of the fundamentals can be set to reproduce the luminous efficiency function (e.g.<sup>12</sup>) or the heights can be normalized to white (e.g.<sup>13</sup>). These choices have different hidden assumptions about the underlying physiology of human color vision. In the first, there is an assumption about the physiological basis of the luminous efficiency function, namely that the luminous efficiency function represents a weighted linear sum of the cone photoreceptor outputs. In the second, there is an assumption about the adaptational properties of the photoreceptor outputs, namely that the three classes of photoreceptor have equal output to the equal-energy spectrum. This assumption implies some form of gain control operating on the photoreceptors.

#### REVISED CHROMATICITY DIAGRAM— JUDD (1951)

The 1931 CIE (**X**, **Y**, **Z**) standard observer for colorimetry combined color-matching data of Wright<sup>14</sup> and Guild<sup>15</sup> with the luminosity data of the 1924 CIE standard observer for photometry. At the time that the Wright and Guild laboratories obtained their data, an absolute radiometric specification of the primaries was not available, although the relative radiance of the test lights was known, as were the relative luminances of the primaries. It was established that the chromaticity coordinates were sufficiently similar to allow averaging, when the two data sets were normalized to the same units. The adequacy of the chromaticity coordinates was later confirmed by Stiles and Burch.<sup>16</sup> Thus, the accuracy of the 1931 CIE (**X**, **Y**, **Z**) standard observer for colorimetry hinges to a great extent on the accuracy of the 1924 CIE standard observer for photometry.

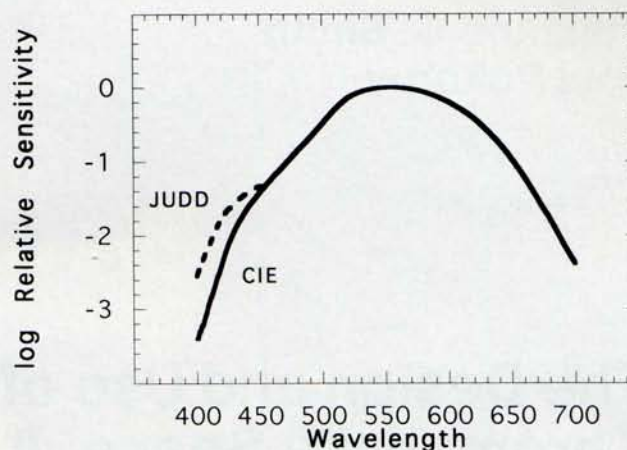


FIG. 1. The luminous efficiency function. A comparison of the CIE 1924 standard observer for photometry with the revised observer proposed by Judd<sup>17</sup> in 1951.

Almost from the acceptance of the 1931 observer for colorimetry, problems attributable to the use of the 1924 observer have been evident.<sup>17</sup> In particular, it appeared that the 1924 standard observer for photometry contained serious errors of underestimation of luminosity at short wavelengths below 460 nm. The 1924 standard observer for photometry was based on data of a number of laboratories.<sup>18–21</sup> Following the earlier work of Ives,<sup>22,23</sup> much of the data used heterochromatic flicker photometry, but also included brightness matching. It is of note that the function did not represent averaged data, but selected data from different laboratories for different parts of the spectrum.<sup>24</sup> The exact method of combination is now lost.<sup>24,25</sup> Since the inadequacy of the  $V(\lambda)$  was recognized to be important in colorimetry, Judd<sup>17</sup> proposed a revised luminous efficiency function,  $V_J(\lambda)$ , which was incorporated with the chromaticity coordinates of the 1931 observer. The revision was based upon a number of studies performed during the 1940s. Figure 1 shows a comparison of the 1924 CIE observer with the Judd revision. Kaiser<sup>24</sup> pointed out that Judd's revision agrees quite well with the average data available to the 1924 committee. The Judd revised colorimetric observer is characterized by less lens and more macular pigment than the CIE 2° observer.<sup>26</sup>

In 1988, the CIE recommended a supplementary observer for photometry, termed  $V_M(\lambda)$ .<sup>25</sup> This observer is principally based on Judd (1951) but includes further revision proposed by Vos.<sup>27</sup> The Vos report, an in-house report of the Instituut voor Zintuigfysiologie, provides 1-nm tabulations for an amended colorimetric observer. It also gives equations to convert from the chromaticity coordinates of the 1931 CIE observer to the chromaticity coordinates of the Judd–Vos observer. In 1978, Vos presented his revised observer<sup>27</sup> with tables at 5-nm intervals. Today, some users continue to use the Judd tabulations, but others use one of the Vos tabulations or use



TABLE I. Copunctal points for Judd-based König Fundamentals used by Smith and Pokorny.

	$x$	$y$
Protanope	0.7465	0.2535
Deuteranope	1.400	-0.400
Tritanope	0.1848	0.0

the Vos equations to derive a Vos tabulation. There are minor discrepancies in calculation among these sets.

The Judd revised colorimetric observer ( $X_J, Y_J, Z_J$ ) was quickly adopted by the Vision community in preference to the CIE 1931 colorimetric observer ( $X, Y, Z$ ).<sup>\*</sup> The first use of the Judd (1951) revised ( $X_J, Y_J, Z_J$ ) chromaticity space was by W. D. Wright. Wright embarked on an intensive search for tritanopic observers in England. In 1952, he published color matching for tritanopes.<sup>29</sup> Tritanopes show confusion colors or metameric test wavelengths, which have identical primary ratios. Confusion colors plotted in chromaticity space intersect at the copunctal point for the dichromat. Thompson and Wright<sup>30</sup> found that the tritan confusion colors converged below the alychne ( $y = 0$ ), in the chromaticity diagram of the 1931 CIE standard observer for colorimetry. This problem was not evident in Judd's revised chromaticity diagram, in which the confusion colors were plotted on or slightly above the alychne. Since it was considered implausible for the SWS cone (or any cone) to have negative luminance, Thompson and Wright derived König fundamentals using the Judd revised observer.

#### JUDD-BASED KÖNIG FUNDAMENTALS—SMITH AND POKORNY

When König fundamentals are derived in the CIE diagram, a consequence of the way the 1931 CIE observer was defined is that  $Z$  represents the spectral sensitivity of the short wavelength sensitive fundamental,  $S$ , (i.e.,  $S = kZ$ ); the primaries of the  $L$  and  $M$  fundamentals fall on the line  $(x + y) = 1$ . This feature of the CIE observer reflects the observation that the short wavelength sensitive photoreceptor has negligible absorption above 550 nm. The color-normal observer is a dichromat when primaries are chosen above 550 nm. This is true not only of the 1931 CIE observer, but also of the Judd (1951) revision and of the 1964 CIE 10° large-field observer for colorimetry.

Table I shows the copunctal points used by Smith and

<sup>\*</sup> Judd used a prime terminology when he introduced his revision:  $\bar{x}'(\lambda)$ ,  $\bar{y}'(\lambda)$ , and  $\bar{z}'(\lambda)$  for the color matching functions and  $x'(\lambda)$ ,  $y'(\lambda)$  for chromaticity coordinates. However, for many the prime terminology connotes the scotopic luminous efficiency function,  $V'(\lambda)$ . The CIE<sup>28</sup> introduced the term  $V_M(\lambda)$  for the revised Judd-Vos luminous efficiency function. In this article we use the subscript  $J$  to refer to the Judd (1951) revised colorimetric observer, ( $X_J, Y_J, Z_J$ ).

Pokorny.<sup>31</sup> These are based on data of the Wright laboratory.<sup>29,32</sup> The normalization was chosen to give heights that would sum to the luminous efficiency function. A feature of the Smith and Pokorny transform, dictated both by psychophysical data<sup>31,33</sup> and by primate electrophysiology,<sup>34</sup> is that the  $L$  and  $M$  fundamentals sum to the luminous efficiency function (i.e.,  $L + M = Y_J$ ). The Smith and Pokorny<sup>31</sup> transformation is a set of equations that relate the color matching functions  $\bar{l}(\lambda)$ ,  $\bar{m}(\lambda)$ ,  $\bar{s}(\lambda)$  to the Judd revised color matching functions,  $\bar{x}_J(\lambda)$ ,  $\bar{y}_J(\lambda)$ ,  $\bar{z}_J(\lambda)$ :

$$\begin{bmatrix} \bar{l}(\lambda) \\ \bar{m}(\lambda) \\ \bar{s}(\lambda) \end{bmatrix} = \begin{bmatrix} 0.15516 & 0.54307 & -0.03287 \\ -0.15516 & 0.45692 & 0.03287 \\ 0.0 & 0.0 & k \end{bmatrix} \begin{bmatrix} \bar{x}_J(\lambda) \\ \bar{y}_J(\lambda) \\ \bar{z}_J(\lambda) \end{bmatrix}, \quad (1)$$

where, according to the requirement for the transformation:

$$\bar{y}_J(\lambda) = \bar{l}(\lambda) + \bar{m}(\lambda). \quad (2)$$

In this transformation, the height of the  $L$  fundamental at its  $\lambda_{\max}$  is 0.6373; that for the  $M$  fundamental at its  $\lambda_{\max}$  is 0.3924. The tritan copunctal point is placed on the alychne. This transform does not yield a scaling for  $S$ ; the value of  $k$  is chosen at the convenience of the user. Figure 2 shows the Smith and Pokorny fundamentals, renormalized to their peaks and plotted on a logarithmic axis. If the three spectral sensitivities are expressed at a retinal level by removing the effects of lens and macular pigment, they are closely similar to measurements made on isolated human cones using a suction electrode technique.<sup>35</sup>

#### CHROMATICITY DIAGRAM—MACLEOD AND BOYNTON

The chromaticity diagram is a projective plane, derived from the color-matching functions. Rather than dividing

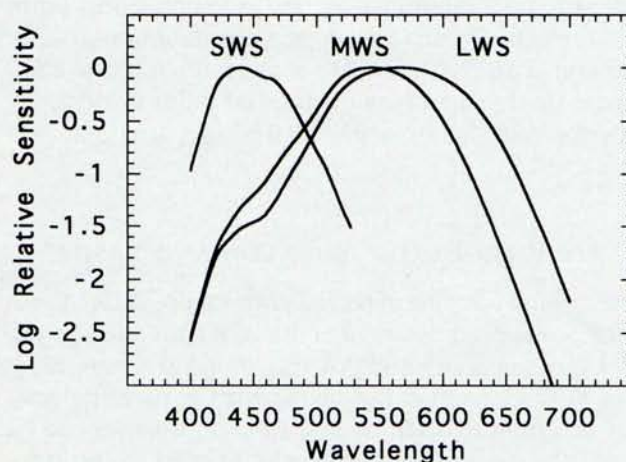


FIG. 2. Smith and Pokorny<sup>31</sup> Judd-based König fundamentals. The fundamentals are shown normalized to peak sensitivity and plotted on an energy basis at the cornea.



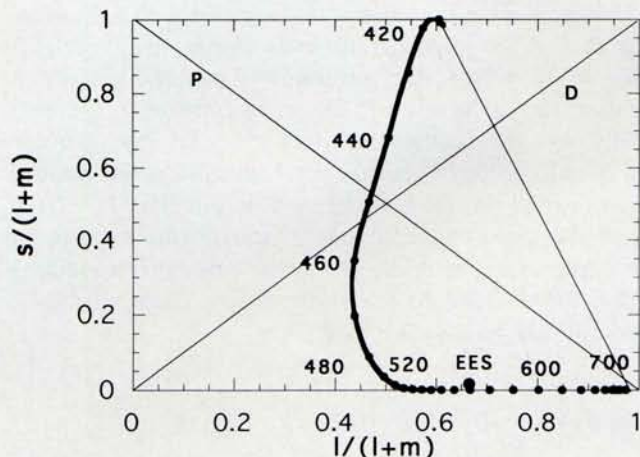


FIG. 3. The rectangular chromaticity diagram proposed by MacLeod and Boynton.<sup>4</sup> This is an equiluminant chromaticity plane. The  $s$ -chromaticity coordinate,  $s/(l+m)$ , is plotted vs. the  $l$ -chromaticity coordinate,  $l/(l+m)$ . Along the horizontal axis,  $l$  and  $m$  are reciprocal. The  $s$ -axis is normalized to have a maximal value of unity.

by the sum of the fundamentals, MacLeod and Boynton<sup>4</sup> proposed a rectangular plane with division by  $Y_J$ , giving an equiluminant chromaticity plane. To ensure a convenient scaling of the diagram, the value of  $k$  was set at 0.01608. With this scaling, the value of  $s(\lambda)/\bar{y}_J(\lambda)$  is unity at 400 nm:

$$\begin{aligned} l(\lambda) &= \bar{l}(\lambda)/\bar{y}_J(\lambda), \\ m(\lambda) &= \bar{m}(\lambda)/\bar{y}_J(\lambda), \\ s(\lambda) &= 0.01608\bar{z}(\lambda)/\bar{y}_J(\lambda). \end{aligned} \quad (3)$$

The MacLeod–Boynton chromaticity diagram includes the specific assumption that  $\bar{z}(\lambda)$  does not contribute to luminance. Figure 3 shows the MacLeod–Boynton chromaticity diagram with  $s(\lambda)$  plotted against  $l(\lambda)$ . The horizontal axis represents the exchange of  $l$ - and  $m$ -luminosity at equiluminance, i.e., an increase in  $l$ -luminosity is offset by an equal decrease in  $m$ -luminosity, but the sum is unity. The protan copunctal point is at coordinate (0, 1); the deutan copunctal point is at (0, 0). Tritan confusions are represented by a set of parallel, vertical lines.

#### CONE TROLANDS—BOYNTON AND KAMBE

The troland is a unit of retinal illuminance defined with reference to the physical definition of light, and, hence,  $V(\lambda)$ . In the Smith and Pokorny transformation, the  $L$  and  $M$  fundamentals can be regarded as part luminosities in summing to  $Y$ .  $L$  and  $M$  cone trolands can be defined as the part luminosities multiplied by the luminance level in trolands. It is less obvious how an  $S$  cone troland should be defined, since  $S$  cones do not contribute to luminance. Boynton and Kambe<sup>36</sup> proposed that

one troland of the equal energy spectrum should yield one  $S$  troland. In specifying cone trolands, Boynton and Kambe substituted the Judd revised  $V_J(\lambda)$  in the physical definition of the troland. Following their use, we define the  $L$ ,  $M$ , and  $S$  cone trolands at wavelength  $\lambda$  as:

$$\begin{aligned} L(\lambda)\text{tds} &= (I_J)\bar{l}(\lambda)/\bar{y}_J(\lambda) = (I_J)l(\lambda), \\ M(\lambda)\text{tds} &= (I_J)\bar{m}(\lambda)/\bar{y}_J(\lambda) = (I_J)m(\lambda), \\ S(\lambda)\text{tds} &= (I_J)\bar{s}(\lambda)/\bar{y}_J(\lambda) = (I_J)s(\lambda), \end{aligned} \quad (4)$$

where  $I_J$  is the retinal illuminance in (Judd-based) trolands,  $k = 1$ , and the other terms are as defined above. A chromaticity diagram may be plotted, normalized to 1 td. Since the spectrum locus at 400 nm has an  $s$ -coordinate value of 62, this normalization may seem inconvenient. However, for real lights that have a limited color gamut, such as those produced on a color video monitor, the relative cone troland space is an effective one.

Colorimetric calculations are easily made using either the MacLeod–Boynton or the Boynton–Kambe spaces. Several examples were given in MacLeod and Boynton.<sup>4</sup> In the Boynton–Kambe relative cone troland space, a light,  $C$ , specified by the Judd revised observer as  $x_J(C)$ ,  $y_J(C)$ ,  $Y_J(C)$  has a unique specification in cone trolands given by  $l(C)$ ,  $s(C)$ ,  $Y_J(C)$ . The tristimulus values,  $L(C)$ ,  $Y_J(C)$ ,  $S(C)$  are calculated in the same way as for  $X_J(C)$ ,  $Y_J(C)$ , and  $Z_J(C)$ . Expression in other primary systems follows the usual rules. For example, to transform between cone trolands and the phosphor outputs of a color monitor, we write:

$$\begin{bmatrix} L(C) \\ Y_J(C) \\ S(C) \end{bmatrix} = \begin{bmatrix} l_1/y_{J1} & l_2/y_{J2} & l_3/y_{J3} \\ 1 & 1 & 1 \\ s_1/y_{J1} & s_2/y_{J2} & s_3/y_{J3} \end{bmatrix} \begin{bmatrix} Y_J(C)_1 \\ Y_J(C)_2 \\ Y_J(C)_3 \end{bmatrix} \quad (5)$$

where the terms  $l_i$ ,  $s_i$  represent the specification in chromaticity coordinates for phosphor ( $i$ ) and  $Y_J(C)_i$  represents the luminance of light  $C$  for phosphor ( $i$ ). Monitor primaries plotted in the relative cone troland diagram are shown in Fig. 4.

#### SPECTRAL OPPONENT SPACE— DERRINGTON, KRAUSKOPF, AND LENNIE

Yet another important transformation of the cone chromaticity space includes a normalization to white and representation of white at the origin of the plot. In this normalization, the  $l$ - and  $s$ -chromaticities are recalculated as  $(l - l_w)$  and  $(s - s_w)$ , the subscript “W” indicates the chromaticity of the white, usually the equal-energy spectrum. This diagram has the axes but not the scaling used by Derrington, Krauskopf, and Lennie.<sup>37</sup> The importance of this diagram in visual science is that it is consonant with the spectral opponency of the Parvocellular pathways of the primate retina and lateral geniculate nucleus. The neutral points of this space were termed the null axes by Derrington, Krauskopf, and Lennie. In the primate parvocellular pathways, there are two major cell



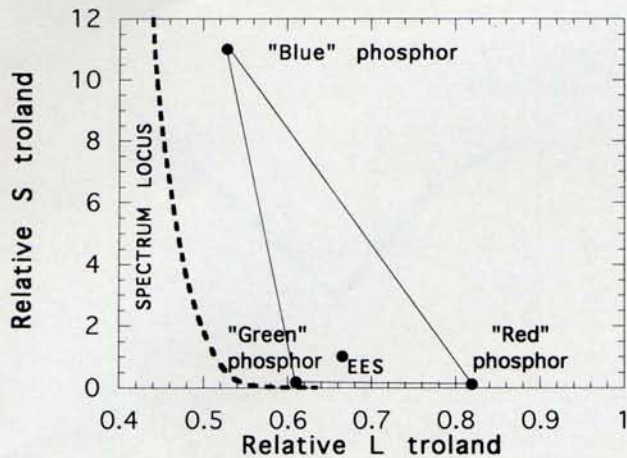


FIG. 4. The chromaticity diagram with a relative cone troland normalization. Primaries of a typical monitor are shown. The heavy solid dashed line shows the portion of the spectrum locus that appears in this format.

classes that show different chromatic signatures.<sup>37-40</sup> Each class contains subsets of cells that differ in center-surround organization and on- or off-center response. The null axes represent the chromatic direction for which equiluminant chromatic modulation does not excite a response in the cell. Figure 5 shows spectral opponent space together with summary data from the Derrington, Krauskopf, and Lennie study. The heavy dashed line is the portion of the spectrum locus that can be plotted. The interpretation of studies of parvocellular chromatic responses is that cells whose null axis coincides with the  $S$ - $Y$  axis receive opponent input from LWS and MWS cones; cells whose null axis coincides with the  $L$ -

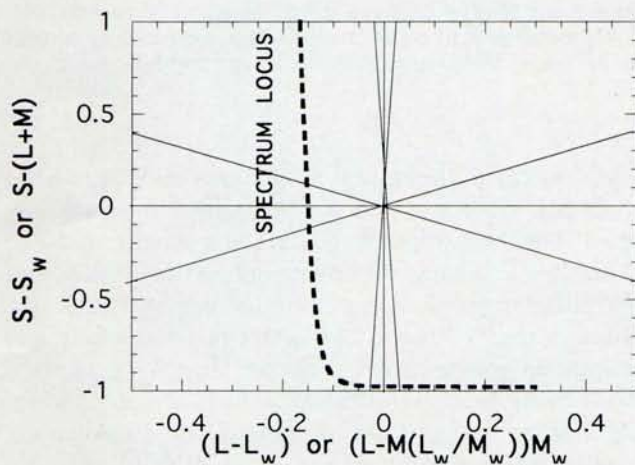


FIG. 5. The chromaticity diagram with a cone-opponent normalization, as proposed by Derrington, Krauskopf, and Lennie.<sup>37</sup> The heavy dashed line shows the portion of the spectrum locus that appears in this format. The bow-tie-shaped regions show the range of null axes reported by Derrington, Krauskopf, and Lennie for cells in the lateral geniculate nucleus of macaque.

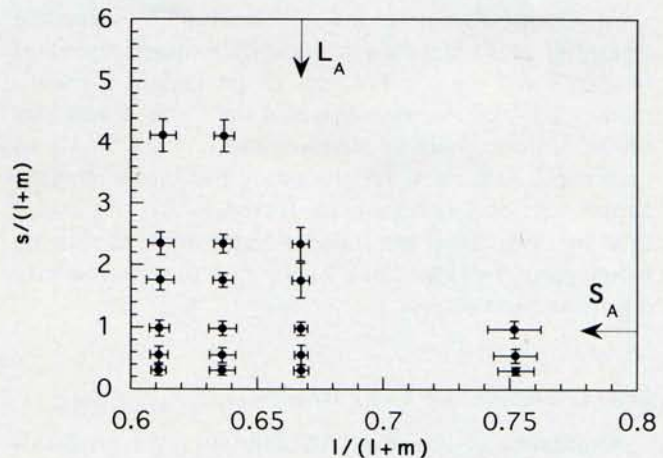


FIG. 6. Equiluminant chromatic discrimination plotted in the relative cone troland chromaticity diagram. The data are for an adapting equiluminant surround ( $l_A$ ,  $s_A$ ) metameric to equal-energy white, indicated by arrows on the figure. Data from Miyahara, Smith, and Pokorny.<sup>41</sup>

$L_w$  axis receive input from the SWS cones opposed by a sum of LWS and MWS cones.

As noted earlier, normalization to white contains an important assumption, namely that the three cone types have all adapted to the chromaticity of the white. For the  $S$  axis, one  $S$  td was defined to be equal to one photopic troland for the equal energy spectrum. Further, in the equiluminant plane,  $Y$  is constant by definition. Thus:

$$(s - s_w) = (s - y) = [s - (l + m)]. \quad (6)$$

For the  $L$  axis,  $(l - l_w)$  can be shown to equal:

$$(l - l_w) = [l - m(l_w/m_w)][m_w]. \quad (7)$$

## CHROMATICITY DISCRIMINATION IN TWO METRICS

The relative cone troland space can directly link chromaticity data with experiments in detection and discrimination. As an example, consider chromaticity discrimination measured using a color monitor, as described in the literature.<sup>41,42</sup> The stimuli are equiluminant and are viewed in an equiluminant surround metameric to equal-energy white. For various starting chromaticities, discrimination steps are measured in both plus and minus  $l$ -directions from the starting  $l$ -chromaticity, and in both plus and minus  $s$ -directions from the starting  $s$ -chromaticity. When the starting chromaticity is identical to the surround, we consider the threshold a detection of a chromaticity change from a background. When the starting chromaticity differs from the surround, we consider the threshold a discrimination.

## Data Expressed in the Relative Cone Troland Chromaticity Diagram

Figure 6 shows the thresholds in the relative cone troland chromaticity diagram. Three factors can be empha-



sized. At any given point in  $(l, s)$  chromaticity space, the threshold  $\Delta l$  is independent of the direction sampled on the  $l$ -axis and the threshold  $\Delta s$  is independent of the direction sampled on the  $s$ -axis. On the  $l$ -axis, thresholds are minimum near the adapting chromaticity,  $l_A$ , and increase to either side. On the  $s$ -axis, thresholds increase as the starting  $s$ -chromaticity increases. To the extent that the two axes are independent, these thresholds would form the minor and major axes for chromaticity discrimination ellipses.

#### Data Expressed in a TVI Format

A different view of the data is the format (threshold-vs.-retinal illuminance or TVI) usually used for increment detection, as exemplified by the experiments of Stiles.<sup>43</sup> In this format, the increment,  $\Delta I$  is plotted as a function of the background illuminance,  $I$ , in logarithmic units. For the data of Fig. 6, this yields two plots of the chromaticity increment, one in  $L$  trolands and one in  $S$  trolands, as in Fig. 7. Now it can be seen that the  $L$  td data form a symmetrical "V" shape about the adapting chromaticity, shown by the arrows marked  $L_A$  and  $S_A$ . The  $S$  td data show a minimum at the adapting chromaticity, but the increase in threshold is asymmetrical, with greater acceleration as  $S$  cone trolands increase. It can be noticed that the horizontal axes of these plots differ, though the vertical axis has the same range. In the equi-luminance plane, the possible variation in  $l$ -chromaticity is less than two-fold; at 100 trolands, the maximal  $L$  troland range is 50–98  $L$  tds. The actual starting chromaticities available on a monitor differ by less than 0.2 log unit. In comparison, the possible variation in  $s$ -chromaticity is much larger. At 100 trolands, the maximal  $S$  troland range is 0–6000 tds. The actual starting chromaticities available on a monitor differ by more than one log unit.

#### CONE EXCITATION UNITS

The cone troland provides an excellent metric for display of chromaticity data. However, yet another unit, the cone excitation unit, is needed for development of physiological models of chromatic processing. Cone excitation units are obtained from cone trolands by dividing by the sensitivity at  $\lambda_{\max}$ :

$$\begin{aligned} L_e(\lambda) &= L(\lambda)/\bar{L}_{\max} \\ M_e(\lambda) &= M(\lambda)/\bar{m}_{\max} \\ S_e(\lambda) &= S(\lambda)/\bar{s}_{\max} \end{aligned} \quad (8)$$

Relative cone excitation units,  $l(\lambda)/\bar{l}_{\max}$ ,  $m(\lambda)/\bar{m}_{\max}$ ,  $s(\lambda)/\bar{s}_{\max}$ , may be used, parallel to relative cone troland units.

Cone excitation units are useful in developing models of spectral opponent processing. The solid lines of Fig. 7 were derived from cone excitation units. In the plots of

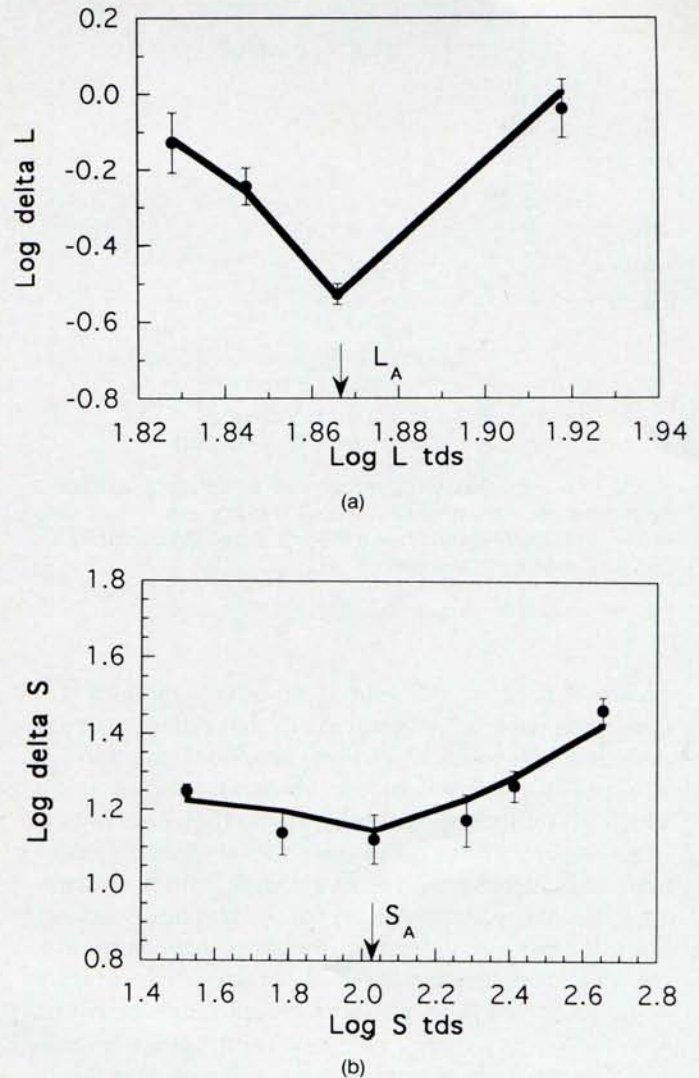


FIG. 7. Equiluminant chromatic discrimination plotted in a TVI format, specified by cone trolands. Panel (a): Data for variation in  $L$  cone trolands. Panel (b): Data for variation in  $S$  cone trolands. The data are for an adapting surround  $[l(A), s(A)]$  metameric to equal-energy white, indicated by arrows on the figure. Data from Miyahara, Smith, and Pokorny.<sup>41</sup>

Fig. 8, we show the results of such modeling applied to chromatic discrimination for the entire luminance domain. For the  $L$  td axis, the data at a fixed luminance show the "V" shape, occupying only a small fraction of the entire troland axis. As luminance increases, the points of the "V" rise to a linear region, characteristic of adaptation gain control. The depth of the "V" is constant in the linear range, but shallows toward absolute threshold. For the  $S$  td axis, the asymmetrical "V" shapes occupy a major portion of the entire troland axis, but change shape with luminance level, becoming shallower as luminance decreases. These models are the type we used to evaluate clinical color vision tests.<sup>44</sup>

As a further example, consider the data of temporal or spatial modulation experiments. In these experiments, the stimuli are usually described in terms of Michelson



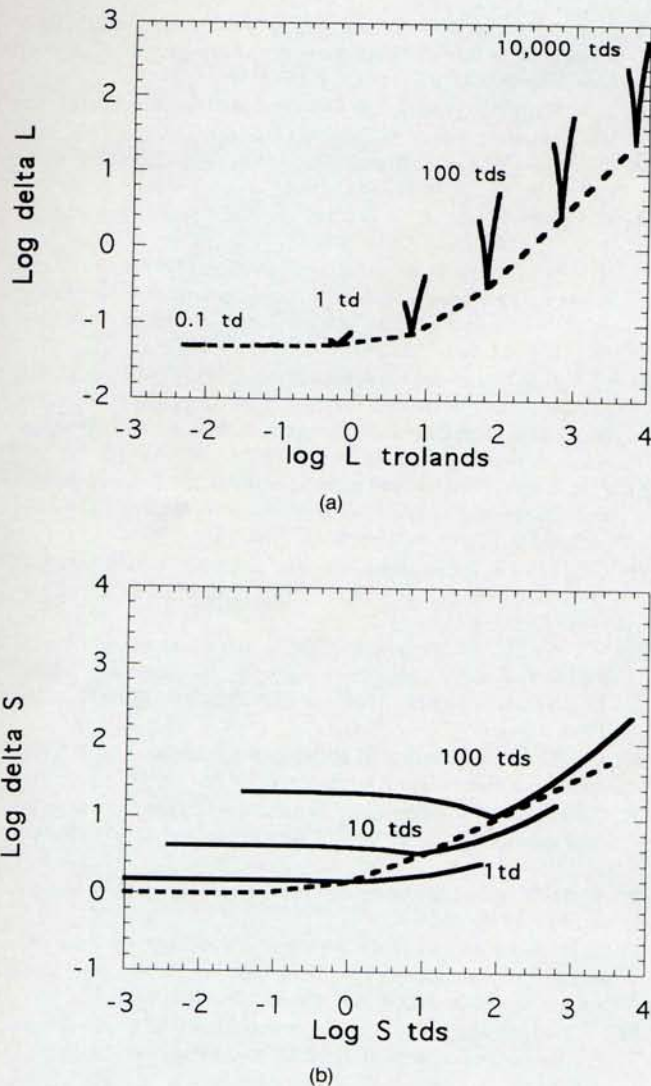


FIG. 8. Predicted chromatic discrimination as a function of chromaticity and luminance. Panel (a): Variation in L cone trolands. Panel (b): Variation in S cone trolands.

contrast.  $(I_{\max} - I_{\min}) / (I_{\max} + I_{\min})$ , where  $I_{\max}$  and  $I_{\min}$  refer to the maximal and minimal excursions of a continuous waveform from its mean level. While this definition is intuitive for luminance modulation, it is less obvious how to relate chromatic modulation to achromatic modulation. For heterochromatic stimuli, modulation between the stimuli is often arbitrarily assigned a physical contrast of 1.00. One solution is to weight physical contrast by the difference in relative cone excitation of the heterochromatic stimuli.<sup>45</sup>

The cone excitation unit has another important property. The quantal excitation rate of the photoreceptors can easily be derived. Quanta,  $Q(\lambda)$  are related to trolands,  $I_\lambda$  at wavelength,  $\lambda$  by the formula:

$$Q(\lambda) = (I/V_J(\lambda))(10^7/8)(\lambda/555). \quad (9)$$

The term  $(10^7/8)(\lambda/555)$  includes the conversion from watts to quanta. The quantal absorption rate for a given

photoreceptor is proportional to the number of quanta multiplied by the fractional absorption spectrum,  $\alpha(\lambda)$  of the photoreceptor. For the LWS photoreceptor, the relative fractional absorption spectrum is related to the relative sensitivity of the fundamental as:

$$\alpha(\lambda)/\alpha(\lambda_{\max}) = k_L(\bar{l}(\lambda)/\bar{l}(\lambda_{\max}))(555/\lambda)/T(\lambda), \quad (10)$$

where  $\alpha_{\lambda_{\max}}$  represents the peak fractional absorption probability of the photopigment *in situ* (usually taken as about 0.4 for a 2° field),  $T(\lambda)$  represents the transmission of the ocular media (lens and macular pigment),  $(555/\lambda)$  converts from the relative energy base of the fundamental to the relative quantal base of an absorption spectrum, and  $k$  is an arbitrary scaling constant to obtain a peak sensitivity of unity. When Eqs. (9) and (10) are combined for each cone type:

$$\begin{aligned} L_Q(\lambda) &= L_e(\lambda)(a_{L_{\max}})(10^7/8)/T(\lambda)k_L \\ M_Q(\lambda) &= M_e(\lambda)(a_{M_{\max}})(10^7/8)/T(\lambda)k_M \\ S_Q(\lambda) &= S_e(\lambda)(a_{S_{\max}})(10^7/8)/T(\lambda)k_S. \end{aligned} \quad (11)$$

Thus for a given cone type, the quantal absorption rate at wavelength,  $\lambda$  is proportional to the cone excitation weighted by constants.

## DISCUSSION

The cone chromaticity space is based on the Judd revised colorimetric observer. In industry, however, it is more common to use either the 1931 CIE standard colorimetric observer or the 1964 CIE large-field colorimetric observer. Is it possible to derive a cone chromaticity space based on either of these observers? Further commercial spectrophotometers and spectroradiometers may give chromaticity coordinates referred to a CIE standard observer. Is it possible to derive cone chromaticity coordinates using CIE chromaticity specification?

There is no general matrix equation to convert between the CIE (1931) and the cone chromaticity space, because Judd's revision is not a linear transform of the 1931 CIE color-matching functions. The transformation equations given by Vos<sup>27</sup> apply only to the chromaticity coordinates representing the spectrum locus.

There is a slightly different problem for the 1964 CIE large-field colorimetric observer. The dichromatic co-punctal points are based on small-field data. There are no corresponding large-field data, because the majority of dichromats do not make dichromatic matches with a large field.<sup>46-48</sup> For color normal observers, the major difference between small- and large-field observers is a variation in macular pigment. Additionally, there is an expected small difference in the shape of the cone absorption spectra due to a lower effective optical density of the photopigments in the large field.<sup>49,50</sup> Because the large-field observer incorporates the important design features that Y is the 10° spectral luminous efficiency



function and  $Z$  is on the alychne, the form of the transformation will follow matrix Eq. (1). We have used the small-field copunctal points to derive König fundamentals for the CIE 10° large-field colorimetric observer using matrix Eq. (1). The resulting fundamentals closely resemble the 2° Smith-Pokorny fundamentals and are probably within the spread of variability of real observer data. Although large-field fundamentals have yet to be evaluated, the application of Eq. (1) to the large-field observer may be useful.

## ACKNOWLEDGMENTS

This article is based on a tutorial presented at the annual meeting of the ISCC, in Greensboro, NC in April, 1995. The work was supported by NEI Research grant EY07390. Publication was supported by an unrestricted grant to the Department of Ophthalmology, University of Chicago from Research to Prevent Blindness.

1. J. C. Maxwell, Experiments on colour, as perceived by the eye, with remarks on colour-blindness, *Trans. Roy. Soc. Edinburgh* **21**, 275–298 (1855).
2. E. Schrödinger, Ueber das Verhältnis der Vierfarben-zur Dreifarben-theorie. Sitzungber. Kaiserl. Wien, Akad. Wiss., *Math.-naturwiss. Kl.* **134**, 471–490 (1925).
3. D. B. Judd, A Maxwell triangle yielding uniform chromaticity scales, *J. Opt. Soc. Am.* **25**, 24–35 (1935).
4. D. I. A. MacLeod and R. M. Boynton, Chromaticity diagram showing cone excitation by stimuli of equal luminance, *J. Opt. Soc. Am.* **69**, 1183–1185 (1979).
5. R. Luther, Aus dem Gebiet der Farbreizmetrik, *Z. Tech. Phys.* **8**, 540–558 (1927).
6. H. von Helmholtz, *Handbuch der Physiologischen Optik*, 2nd Ed., Voss, Hamburg, 1896.
7. J. Pokorny, V. C. Smith, G. Verriest, and A. J. L. G. Pinckers, Eds. *Congenital and acquired color vision defects*, Grune and Stratton, New York, 1979.
8. A. König and C. Dieterici, Die Grundempfindungen und ihre Intensitäts-Vertheilung im Spectrum, *J. Sitz Akad Wiss* (Berlin), **2**, 805–829 (1886).
9. A. König and C. Dieterici, Die Grundempfindungen in normalen und anomalen Farben Systemen und ihre Intensitäts-Vertheilung im Spectrum, *Z. Psychol. Physiol. Sinnesorg.* **4**, 241–347 (1893).
10. G. S. Brindley, *Physiology of the Retina and the Visual Pathway*, Ed. 2, Williams & Wilkins, Baltimore, 1970.
11. V. C. Smith and J. Pokorny, Spectral sensitivity of color-blind observers and the human cone photopigments, *Vision Res.* **12**, 2059 (1972).
12. J. J. Vos and P. L. Walraven, On the derivation of the foveal receptor primaries, *Vision Res.* **11**, 799–818 (1971).
13. D. B. Judd, Response functions for types of vision according to the Mueller theory, *J. Res. Nat. Bur. Stand. (USA)* **42**, 1–16 (1949).
14. W. D. Wright, A re-determination of the trichromatic coefficients of the spectral colours, *Trans. Opt. Soc.* **30**, 141–164 (1929).
15. J. Guild, The colorimetric properties of the spectrum, *Phil. Trans. Roy. Soc. London A* **230**, 149–187 (1931).
16. W. S. Stiles and J. M. Burch, Interim report to the Commission Internationale de l'Eclairage, Zurich, 1955, on the National Physical Laboratory's investigation of colour-matching, *Optica Acta* **2**, 168–181 (1955).
17. D. B. Judd, Colorimetry and artificial daylight, in *Technical Committee No. 7 Report of Secretariat United States Commission, International Commission on Illumination, Twelfth Session, Stockholm, 1951*, pp. 1–60.
18. W. W. Coblentz and W. B. Emerson, Relative sensibility of the average eye to light of different colors and some practical applications, *Bur. Stand. (U.S.) Bull.* **14**, 167–236 (1917).
19. L. W. Hartman, Visibility of radiation in the blue end of the visible spectrum, *Astrophys. J.* **42**, 83–95 (1918).
20. E. P. Hyde, W. E. Forsythe, and F. E. Cady, The visibility of radiation, *Astrophys. J.* **48**, 65–88 (1918).
21. K. S. Gibson and E. P. T. Tyndall, The visibility of radiant energy, in *Sci. Pap. Nat. Bur. Stand.* **475**, 131–191 (1923).
22. H. E. Ives, Studies in the photometry of lights of different colours, I. Spectral luminosity curves obtained by the equality of brightness photometer and the flicker photometer under similar conditions, *Phil. Mag.* **24**, 149–188 (1912).
23. H. E. Ives, Studies in the photometry of lights of different colours, III. Distortions in spectral luminosity curves produced by variations in the character of the comparison standard and of the surrounding photometric field, *Phil. Mag.* **24**, 744–751 (1912).
24. P. K. Kaiser, Photopic and mesopic photometry: Yesterday, today and tomorrow, in *Golden Jubilee of Colour in the CIE*, The Society of Dyers and Colourists, Bradford, 1981.
25. CIE, Light as a true visual quantity: principles of measurement, *Publ. CIE No. 41 (TC-1.4)*, Bureau Central de la CIE, Paris, (1978).
26. V. C. Smith, J. Pokorny, and Q. Zaidi, How do sets of color-matching functions differ?, in *Colour Vision: Physiology and Psychophysics*, J. D. Mollon and L. T. Sharpe, Eds., Academic Press, London, 1983, 93–105.
27. J. J. Vos, Colorimetric and photometric properties of a 2° fundamental observer, *Color Res Appl.* **3**, 125–128 (1978).
28. CIE, CIE 1988 2° spectral luminous efficiency function for photopic vision, *Publ. CIE No. 86*, Bureau Central de la CIE, Paris (1990).
29. W. D. Wright, The characteristics of tritanopia, *J. Opt. Soc. Am.* **42**, 509–520 (1952).
30. L. C. Thomson and W. D. Wright, The convergence of the tritanopic confusion loci and the derivation of the fundamental response functions, *J. Opt. Soc. Am.* **43**, 890–894 (1953).
31. V. C. Smith and J. Pokorny, Spectral sensitivity of the foveal cone photopigments between 400 and 500 nm, *Vision Res.* **15**, 161–171 (1975).
32. F. H. G. Pitt, The nature of normal trichromatic and dichromatic vision, *Proc. Royal Soc.* **132B**, 101–117 (1944).
33. A. Eisner and D. I. A. MacLeod, Blue sensitive cones do not contribute to luminance, *J. Opt. Soc. Am.* **70**, 121–123 (1980).
34. B. B. Lee, P. R. Martin, and A. Valberg, Sensitivity of macaque retinal ganglion cells to chromatic and luminance flicker, *J. Physiol. (London)* **414**, 223–243 (1989).
35. J. L. Schnapf, T. W. Kraft, and D. A. Baylor, Spectral sensitivity of human cone photoreceptors, *Nature* **325**, 439–441 (1987).
36. R. M. Boynton and N. Kambe, Chromatic difference steps of moderate size measured along theoretically critical axes, *Color Res. Appl.* **5**, 13–23 (1980).
37. A. M. Derrington, J. Krauskopf, and P. Lennie, Chromatic mechanisms in lateral geniculate nucleus of macaque, *J. Physiol. (London)* **357**, 241–265 (1984).
38. T. Wiesel and D. H. Hubel, Spatial and chromatic interactions in the lateral geniculate body of the rhesus monkey, *J. Neurophysiol.* **29**, 1115–1156 (1966).
39. R. L. DeValois, I. Abramov, and G. H. Jacobs, Analysis of response patterns of LGN cells, *J. Opt. Soc. Am.* **56**, 966–977 (1966).
40. B. B. Lee, A. Valberg, D. A. Tigwell, and J. Tryti, An account of responses of spectrally opponent neurones in the macaque lateral geniculate nucleus to successive contrast, *Proc. Roy. Soc. B* **230**, 293–314 (1987).
41. E. Miyahara, V. C. Smith, and J. Pokorny, How surrounds affect chromaticity discrimination, *J. Opt. Soc. Am. A* **10**, 545–553 (1993).



42. Q. Zaidi, A. Shapiro, and D. Hood, The effect of adaptation on the differential sensitivity of the S-cone color system, *Vision Res.* **32**, 1297-1318 (1992).
43. W. S. Stiles, Color vision: The approach through increment threshold sensitivity, *Proc. Natl. Acad. Sci. USA* **45**, 100-114 (1959).
44. V. C. Smith, J. Pokorny, and T. Yeh, Pigment tests evaluated by a model of chromatic discrimination, *J. Opt. Soc. Am. A* **10**, 1773-1784 (1993).
45. V. C. Smith, B. B. Lee, J. Pokorny, P. R. Martin, and A. Valberg, Responses of macaque ganglion cells to the relative phase of heterochromatically modulated lights, *J. Physiol. (London)* **458**, 191-221 (1992).
46. V. C. Smith and J. Pokorny, Large-field trichromacy in protanopes and deuteranopes, *J. Opt. Soc. Am.* **67**, 213-220 (1977).
47. M. Breton and W. Cowan, Deuteranomalous color matching in the deuteranopic eye, *J. Opt. Soc. Am.* **71**, 1220-1223 (1981).
48. A. L. Nagy, Large-field substitution Rayleigh matches of dichromats, *J. Opt. Soc. Am.* **70**, 778-784 (1980).
49. J. Pokorny, V. C. Smith, and S. J. Starr, Variability of color mixture data—II. The effect of viewing field size on the unit coordinates, *Vision Res.* **16**, 1095-1098 (1976).
50. J. Pokorny and V. C. Smith, Effect of field size on red-green color mixture equations, *J. Opt. Soc. Am.* **66**, 705-708 (1976).

Received 2 October 1995; accepted 9 January 1996